

Effects of the Controlled Underexpression of IGFBP7 through the Drug Sacubitril/Valsartan for Geriatric Diseases

Tony Gao

The Webb School of California, Claremont, United States

Email: tonygao@webb.org

Abstract—Geriatric diseases account for approximately 75% of all deaths since the 20th century. Despite their apparent diversity, these conditions may share common upstream mechanisms. This study investigates the upstream mechanisms of cellular aging and their connections to geriatric diseases through the analysis of Sacubitril/Valsartan, a novel drug for Heart Failure with preserved Ejection Fraction (HFpEF), on Insulin Growth Factor Binding Protein 7 (IGFBP7). Preliminary computational modeling using AutoDock Vina displayed binding affinities of -6.2 and -5.4 kcal/mol for Sacubitril and Valsartan, respectively, with IGFBP7, surpassing the average binding affinity of -4.6 kcal/mol for five control drugs. Protein-ligand interaction profiling identified eight hydrophobic interactions, two hydrogen bonds, and one salt bridge in the complex. Further binding site analysis determined the most probable binding site near amino acid 155 in the IGFBP7 sequence. To further elucidate the role of IGFBP7, a Bayesian probabilistic network analyzed heart failure datasets from the GEO database, indicating significant IGFBP7 upregulation in 89% of heart failure patients, with 97% of the fourth quartile exhibiting heart failure. A similar machine learning analysis of cerebral endothelial datasets in post-MCAO mice revealed that $> 87.4\%$ of stroke cases belonged to the highest quartile of IGFBP7 expression, with an over threefold increase compared to the controls. Complementing computational and statistical findings, in-vitro experiments were conducted using primary brain microvascular endothelial cells (C57BL/6 with Sacubitril/Valsartan at 0, 20, 40, and 60 μM under normoxic and hypoxic conditions. Cell viability assays determined an IC_{50} of ~ 55 μM , with hypoxic conditions reducing viability. These results suggest Sacubitril/Valsartan's potential to modulate apoptosis and influence vascular aging. These findings identify IGFBP7 as a potential upstream factor in geriatric diseases and highlight its therapeutic potential as a target for vascular drugs like Sacubitril/Valsartan.

Keywords—bioinformatics, geriatric diseases, IGFBP7

I. INTRODUCTION

Many diseases seem separate but may possess a general cause around the occurrence of them. In this article, connections are drawn through biological pathway

analysis as well as an analysis of a specific gene known as Insulin Growth Factor Binding Protein 7, or IGFBP7, which creates the IGFBP7 protein. The IGFBP7 protein is 27 kD protein inside of the senescence secretome [1]. This gene in particular has shown correlations between a crucial part of aging and geriatric diseases, cellular senescence, and is a frequent occurrence of upregulation within vascular related geriatric diseases. IGFBP7 is connected with a variety of pathways, the majority of them related with cellular growth and development. It is correlated with the TGF Beta pathway, which promotes cellular growth [2] and division as well as being connected with the mcf-7 cellular proliferation [3], the BNP3L pathway [4], inhibition of the enzyme neprilysin, BRAF signaling [5], R-HSA-2559583 [6] cellular senescence pathway, and causes LOXL4 oxidative stress activation [7]. These connections show correlation as well as causality of the gene IGFBP7 and cellular senescence, which in turn also correlates with aging as a concept. Sacubitril /Valsartan (brand name Entresto) is a first-in-class Angiotensin Receptor Neprilysin Inhibitor (ARNI) that combines the neprilysin inhibitor sacubitril with the Angiotensin Receptor Blocker (ARB) valsartan to target multiple pathways involved in heart failure pathophysiology, specifically Heart Failure with preserved Ejection Fraction (HFpEF). Sacubitril inhibits neprilysin, an enzyme that degrades vasoactive peptides such as natriuretic peptides, and bradykinin. By preserving these peptides, sacubitril promotes vasodilation, natriuresis, and anti-fibrotic effects [8]. On the other hand, Valsartan blocks the angiotensin II type 1 receptor, counteracting the harmful effects of an overactive Renin-Angiotensin-Aldosterone System (RAAS). This action further results in vasodilation, reduced aldosterone secretion, and decreased cardiac remodeling [8]. The primary hypothesis within this research is to prove if IGFBP7 is an upstream factor within geriatric diseases with its downregulation bringing positive effects towards geriatric diseases (stroke) and aging through its interactions with Sacubitril/Valsartan. IGFBP7 is shown to be an active biomarker in a multitude of geriatric diseases. Some downsides to the controlled underexpression of IGFBP7 would be its potential kidney problems, which also relates to why the drug Sacubitril/Valsartan has a roughly 5% likelihood to

cause kidney failure [9]. Sacubitril/Valsartan acts upon IGFBP7 contrary to regular Valsartan, demonstrating its benefits for HFpEF. This study shows how treatment using Sacubitril/Valsartan affects the recovery of patients afflicted by HFpEF, concluding that Sacubitril/Valsartan does indeed downregulate IGFBP7 and can be used as a potential drug to target IGFBP7 in other cases of overexpression. A study analyzing the mechanisms of IGFBP7 and how it relates to the Htra3-TGFB-IGFBP7 axis, which in turn effect cardiac fibroblasts which regulate the development of HF. Another paper regarding the effects of IGFBP7 and HF demonstrates how IGFBP7 regulated senescence pathways promotes cardiac inflammatory injury, tissue fibrosis, and cardiac senescence as well as the contrary that reduced IGFBP7 was beneficial towards the recovery of HF [10, 11]. The connection IGFBP7 has with other geriatric diseases is further elaborated on in its presence within TBI, where it is shown that IGFBP7 is upregulated within many diseases, such as stroke, another geriatric disease [12]. This upregulation within stroke cells may contribute to the excess cellular apoptosis that occurs after a stroke is experienced, and is this research's next topic to analyze. In order to better understand the mechanism behind healing post-stroke afflicted cells, a protein-ligand complex was created to find the binding affinities and locations of bonds for the complex of Sacubitril/Valsartan and IGFBP7 as well as a Bayesian Probabilistic Network to affirm the correlation and causation between the expression and diseases.

II. MATERIALS AND METHODS

A. Used Datasets

The datasets used for the Bayesian network are commercially available and can be found on the GEO (GSE168742) [13]. The GEO is a database provided by the National Center of Biotechnology Information and is an open source database. The datasets used for this experiment were two CSV files, one regarding patients with HF and another control sample.

B. Autodock Modelling

The IGFBP7 protein was downloaded off of AlphaFold (Uniprot:Q16270). This protein was then converted into a pdb using Pymol in order for it to be able to be accessed by Autodock Vina and MGLtools. After this process, the protein is then imported into Autodock MGLtools where it is prepared for modeling. This preparation includes deleting all water molecules so they do not affect the protein, adding polar hydrogens, and adding Kollman charges. After this, the molecule is selected as a protein in MGLtools and exported as a pdbqt in order for Vina to be able to analyze it. A similar process for the ligand is conducted but with a few alterations to the procedure. The ligand Sacubitril was downloaded off Pubchem, and imported onto Pymol in order for it to be exported as a pdb. After this, the ligand is imported to Autodock

MGLtools in order for ligand preparation to proceed. The preparation process first selects the ligand within MGLtools, then adds Gasteiger charges, merges non-polar hydrogens, detects rotatable bonds, detects aromatic carbons, and sets the TORSDOF to 10 for Valsartan and 13 for Sacubitril. After this process is done, the file is exported as a pdbqt, and then loaded onto a different file with the protein on it. Inside this file, first initialize the ligand as the ligand that will be used and the protein as the protein that will be used. After this is done, set up a gridbox using "Grid" around the area where it is most likely to dock, in this case, around sequence number 158. The binding site is found using a variety of different methods. Firstly, a concentration analysis of the protein on the Prankweb machine learning P2rank software to determine the general area of the binding site [14]. Double check the area using COACH analysis to confirm the general area of the findings. Then using PrDOS which detects disorderly regions of the protein to help pinpoint where the binding site will be. All three analysis options pointed towards the binding site being around number 158 on the protein sequence. Repeat this process for Valsartan and then use Autodock Vina to analyze. In order to properly use Autodock Vina, first set the protein in the code to be "the name of the protein".pdbqt, in this case, IGFBP7.pdbqt. Set the ligand in the same way and create a config.txt file, a log.txt file, and run the code on Vina.

C. Bayesian Probabilistic Model

The model used for this research was a Bayesian Probabilistic Network, which allows for the determination of specific probabilities through separate datasets. The reasoning behind the use for this model is to string together multiple, separate, datasets to find the probability that overexpressed IGFBP7 impacts specific geriatric diseases. In this paper, this Bayesian network is applied to two datasets of IGFBP7 expression in HFpEF and post-MCAO mice. The resulting data was separated into two ways, one directly showing the probability of a disease with upregulated IGFBP7, and the other separating IGFBP7 into four quartiles with their respective probabilities. Upregulated IGFBP7 was discretized into binary using two methods. First, discretizing the dataset using a general level of the peak of the control, in this case around 140. The second method was to separate the data into four quartiles in accordance with the general levels of IGFBP7 expression and then analyze that in four categories. All programs were created using Python and Bnlearn through VSC [15].

D. Modelling Setting

The experiments were all conducted on a personal computer with 64 gigabytes of RAM. Ligand models were downloaded off PubChem and compiled using MGLTools. The protein model was first downloaded off of AlphaFold (Fig. 1), then exported into Pymol to convert it into a pdb and prepared using MGLTools.

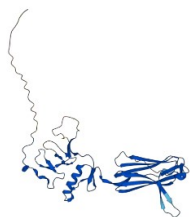


Fig. 1. AlphaFold protein structure of IGFBP7 in Homo Sapien.

E. In-Vitro Experimentation

1) Materials

Valsartan/LBQ: Obtained from Novartis Pharma AG or MedChemExpress (LCZ696) [16, 17], Mouse Endothelial Cells: C57BL/6 Mouse Primary Brain Microvascular Endothelial Cells (Catalog No. C57-6023) from Cell Biologics [18], DMSO, 96 Well Plates, SRB Dye, Hypoxia Workbench (X3 Xvivo System, BioSpherix, NY, USA) [19].

2) Methods

To prepare the Valsartan/LBQ solution, the compound is dissolved in 100% Dimethyl Sulfoxide (DMSO) to achieve a final concentration of 10 mmol/L. Once prepared, the solution is stored at -80°C until required for experimentation [18]. Mouse endothelial cells, derived from C57BL/6 or regular Mus musculus strains, are utilized in this study. The cells are seeded into two 96-well plates at a density of 200 μL per well. Following seeding, the plates are incubated for 0.5 hours to allow the cells to acclimate and adhere to the wells. For the drug treatment phase, the prepared Valsartan/LBQ solution is diluted in the cell culture medium to achieve final concentrations of 0, 20, 40, and 60 μM . These varying concentrations are applied to the cells in the 96-well plates. The cells are incubated with the drug for a total of 20 hours, with periodic assessments conducted at 4-hour intervals, as necessary. After the incubation period, the plates are frozen, and the cells are washed and stained using SRB dye to facilitate subsequent analysis. The final analysis involves the use of a plate reader to evaluate cell death relative to untreated control groups. Data collected during this phase are used to calculate the half-maximal inhibitory concentration (IC_{50}) and other potency metrics, providing insights into the drug's efficacy.

III. RESULTS

This section will cover the results of this research including the binding affinities of the Autodock Vina modeling, the binding site analysis and the multiple different methods used to achieve it, a Bayesian network probability results and graphs of the distribution for the data within the GEO Dataset for heart failure and stroke, and an in-vitro experiment on mus musculus primary endothelial cells.

A. Binding Affinity and Site Modelling

The binding affinity of the IGFBP7-Sacubitril/Valsartan protein-ligand complex was created using Autodock Vina. This process required two separate

models to be constructed, as Vina did not have a way to analyze both ligands at once. These complexes were the docked output of the Vina modeling and visualized on Pymol. The creation of these two complexes was using the program Autodock MGLtools, which allowed for the preparation of the protein and ligand for docking, and was output by Vina (Fig. 2). Accuracy for the Autodock Vina was affirmed using testing through multiple different iterations of testing. Five different ligands were used to ensure the results of Sacubitril/Valsartan were indeed unique.

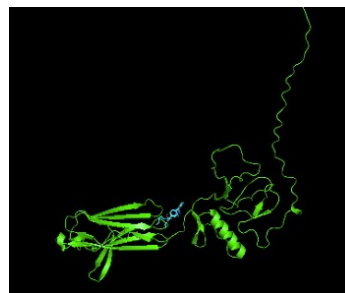


Fig. 2. Valsartan-IGFBP7 docked protein-ligand complex.

Vina exported 9 different possible poses/modes the ligand could be in during the binding process with respective binding affinities for both Valsartan and Sacubitril with the most probable binding affinity being 5.6 kcal/mol for Valsartan and 6.2 kcal/mol for Sacubitril (Fig. 3). During the analysis of the data, only the first mode was considered, as it is the most probable. This data was constructed using proteins and ligands created and prepared using MGLtools, and were altered in order to prepare them and set an environment for binding.

mode	affinity (kcal/mol)	dist from best mode rmsd l.b. rmsd u.b.
1	-6.2	0.000 0.000
2	-6.1	1.886 8.576
3	-6.0	1.383 2.394
4	-5.8	3.086 10.108
5	-5.8	3.185 9.038
6	-5.8	3.470 9.033
7	-5.6	18.592 21.387
8	-5.5	3.005 4.034
9	-5.5	2.741 4.994

Fig. 3. Sacubitril-IGFBP7 Autodock Vina binding affinity analysis.

Additional testing was done to confirm Sacubitril/Valsartan as being different from any other ligand through the testing of Isosorbide, Aspirin, Lisinopril, Acetaminophen, and Ibuprofen, with an average binding affinity of 4.52 kcal/mol, around a 1.48 kcal/mol difference from Sacubitril/Valsartan. The method to determine the binding site of the protein-ligand interaction was by using the program PrankWeb (Fig. 4) to model and analyze the protein IGFBP7 using the P2rank machine learning program to discover pocket regions of the protein where ligands could bind [17]. The figure shown below is the Prankweb visualization of the protein with its levels of conservation indicating a higher likelihood of binding. This binding site is around amino acid number 158 on IGFBP7's sequence.

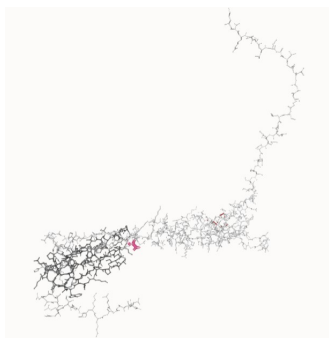


Fig. 4. Prankweb analysis of most probable binding sites for Valsartan on IGFBP7 through sequence concentrations.

This result was concluded due to high conservation in the sequence of IGFBP7. Conservation is especially important as they tell which areas of a protein are more viable for potential binding. Additional confirmations for this result were made using COACH, a meta-server method using TMSite and S-Site, which recognizes ligand binding templates using the BioLiP database, the result of which is seen in Fig. 5 [20].

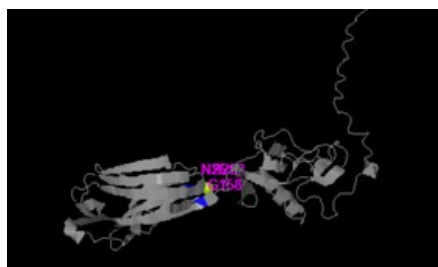
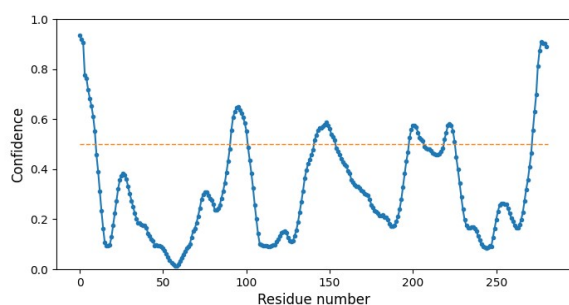


Fig. 5. COACH analysis of IGFBP7 to determine the location of the binding site.



1	MERPPRALLL	GAAGLLLLLL	PLSSSSSSDA	CGPCVPASCP	ALPRLGCPGL	50
51	ETRDAGCCCP	VCARGECEPC	GGGAAGRGHC	APGMECVKSR	KRRKGKAGAA	100
101	AGGPATLAVC	VCKSRYPVCG	SNGITYPSGC	QLRAASLRAE	SRGEKAITQV	150
151	SKGTCEQGGS	IVTPPKDIWN	VTGAKVFLSC	EVIGIPTPVL	IWNKVCRDHS	200
201	GVQRTELLPG	DRENLAIQTR	GGPEKHEVTG	WVLVSPLSKE	DAGEYECHAS	250
251	NSQGQASAAA	KITVVDALHE	IPLKKGEQAQ	L		300

Fig. 6. PrDOS analysis on the protein IGFBP7 to determine probable binding sites through disorderly areas of the protein (above). The list below is a PrDOS analysis on the sequence for IGFBP7 which outputs disorderly regions most receptive of a ligand.

This binding site is further supported with another result using PrDOS (Protein DisOrder prediction System), which predicts disorderly regions of the protein which are more likely to bond. The results of this analysis demonstrate a spike at around the high 150's region of the amino acid sequence (Fig. 6) with these combined respective results showing a strong probability that the

binding site of IGFBP7 will be around the high 150 areas of the protein sequence. Combined with the fact that the Autodock docking output of the Vina experiment showing that the ligand docked in around the same area, it is extremely likely that the binding site of IGFBP7 is in this general area.

B. Binding Site Mechanisms and Toxicology

To analyze the binding mechanisms behind the protein ligand interaction of IGFBP7 and Sacubitril/Valsartan, analysis using the PLIP software showed hydrogen bonds, hydrophobic interactions, and salt bridges. This process was done individually in both Sacubitril and Valsartan. This PLIP analysis demonstrates significance in showing the structure of how the protein binds to the ligand. This can be seen as a up close visualization of the binding process that occurs at the binding site. This analysis also demonstrates how different charges, ions, and waters interact between the protein and the ligand, giving a better picture of how the protein ligand interaction works and takes place. This same test was done using Sacubitril giving a couple of different results. Sacubitril had a different number of hydrogen bonds, different hydrophobic interactions with instead of 162A, one was at 117A and did not have any hydrophobic interactions at 224A. Sacubitril and Valsartan did have some similar hydrophobic interactions at 185A, 225A, though there is a difference between the amount of times these interactions occurred within the two interactions.

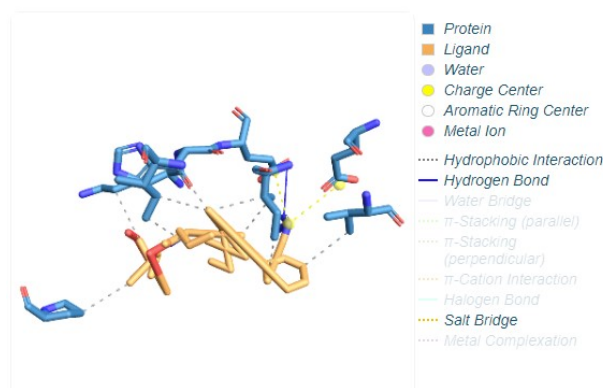


Fig. 7. PLIP analysis on an IGFBP7 – Sacubitril protein ligand complex which shows the interactions between Sacubitril and IGFBP7 including hydrophobic interactions, waters, charge centers, hydrogen bonds, etc.

The results given by PLIP analysis (Fig. 7) for Sacubitril showed 9 hydrophobic interactions, 3 hydrogen bonds, and a mean distance between binding at 3.7 Å. Valsartan, on the other hand, also has 9 hydrophobic interactions but only has one hydrogen bond and has two salt bridges. The median distance of the hydrophobic interactions was also 3.7 Å. Lastly, toxicology analysis was performed using LAZAR toxicology software and due to lacking samples of similar compounds, some results couldn't be computed. The best we have is a compound with roughly 23% similarity in structure being non-carcinogenic, which can be seen in Fig. 6. Sacubitril/Valsartan is also a compound that has been tested through clinical trials and has shown little to effect to the BBB.

C. Bayesian Network on HFpEF

Upregulation of IGFBP7 within HF was confirmed through a Bayesian probabilistic network created using VSC. The dataset used for this was found on GEO (GSE168742) a database created by the National center of biotechnology information. The results show that roughly 89% of all patients with upregulated IGFBP7 in the study were afflicted by HF. This result indicates a strong correlation between IGFBP7 upregulation and HFpEF. The distribution of IGFBP7 within the dataset was also analyzed between the combined dataset of the disease and control, demonstrating a significant difference in expression between the two datasets (Fig. 8). The average IGFBP7 concentration within the dataset of patients with HF is at around 390 FPKM, while the control sample sat at around 89 FPKM. This displays a 4.38 times difference within upregulation of expression within the sample.

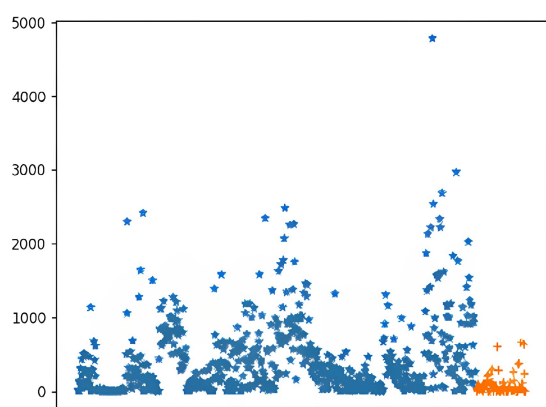


Fig. 8. Scatter plot of IGFBP7 spread within patients with heart failure with ejection fraction (blue) and without (orange).

Upregulation of IGFBP7 within HF was also displayed by an analysis in quartiles. This analysis was also performed using VSC and shows a significant amount of patients being at the highest level of IGFBP7 upregulation, the fourth quartile. This fourth quartile has roughly 50% of the patients who are afflicted with HF and around 97% of patients with IGFBP7 in the fourth quartile are afflicted with HF showing an upwards trend (Fig. 9). This upwards trend means that higher levels of IGFBP7 can be an indicator of higher likelihood of HF or other related geriatric diseases.

IGFBP7	IGFBP7(1)	IGFBP7(2)	IGFBP7(3)	IGFBP7(4)
Heart Failure(0)	0.21037463976945245	0.0	0.038461538461538464	0.027247956403269755
Heart Failure(1)	0.7896253602305475	1.0	0.9615384615384616	0.9727520435967303

Fig. 9. CPD of Bayesian probabilistic network in four distinct quartiles of HF based on expression of IGFBP7 indicating a strong positive correlation between IGFBP7 and HFpEF.

These results are significant due to the correlation and causation, it brings and determines between IGFBP7 and geriatric diseases as well as displaying a potential therapeutic method to help those afflicted. Upregulation of IGFBP7 within stroke was also confirmed using a

Bayesian probabilistic network. This was created in a similar fashion for the HF Bayes Network by quartiles. The dataset used to run the code on was found on the GEO (221379) SRA run which dropped the data off in a sra.lite format within a GCP bucket. This data was further transformed into a fastq format through the use of Sratoolkit through console. The fastq file was finally transformed into FPKM and TPM gene expressions through Basepair, an NGS data analysis tool. The quality of the gene expression reads sat at 97.3% and 95.9% as seen below.

This data analysis has a major flaw however in the compression of fastq data into a singular averaged gene expression which greatly decreased the amount of available sample data that can be used for the Bayesian network processing. The probability results for IGFBP7 being within the fourth quartile of stroke sat at higher than 87.4% while the overwhelming majority of cases within control patients possessed IGFBP7 within the normal first quartile. The average FPKM expression within a control subject was at around 86.1007 FPKM while a subject afflicted with stroke possessed around 285.4475 FPKM, an over 3.3 times upregulation within the stroke sample (Table I).

TABLE I. COMPLETE CPD OF BAYESIAN NETWORK PERFORMED ON A MICE STROKE MICROVESSEL EXPRESSION DATASET (GSE221379) IN QUARTILES

Name	Q1	Q3	Q4	Avg FPKM
Stroke (0)	> 99%	< 1%	< 1%	86.1007
Stroke (1)	< 1%	< 12.6%	> 87.4%	285.4475

Preliminary experiments indicated that Valsartan/LBQ potentially inhibits apoptosis in mouse endothelial cells in a dose-dependent manner. However, these results should be interpreted cautiously, as further replication and validation are necessary to confirm these observations. The impact of Valsartan/LBQ on cell viability was assessed at varying concentrations (Table II). The results, presented as percentages of the untreated control, showed a clear dose-dependent decrease in cell viability.

TABLE II. IN-VITRO CELL VIABILITY ASSAY ACROSS VARIOUS CONCENTRATIONS WITH CONTROL MOUSE ENDOTHELIAL CELLS UNDER NORMOXIC CONDITIONS

Concentration (μ M)	Cell Viability (% of Control)
0	100
20	80
40	65
60	50

The calculated IC₅₀ value for Valsartan/LBQ in these experiments was approximately 55 μ M, indicating moderate potency in reducing cell viability under the experimental conditions. To simulate physiological stroke-like stress, experiments were conducted under hypoxic conditions. The results demonstrated a similar dose-dependent trend with a slightly enhanced reaction in cell viability compared to normoxic conditions (Table III).

TABLE III. IN-VITRO CELL VIABILITY ASSAY ACROSS VARIOUS CONCENTRATIONS WITH CONTROL MOUSE ENDOTHELIAL CELLS UNDER HYPOXIC CONDITIONS

Concentration (μ M)	Cell Viability (% of Control)
0	100
20	85
40	70
60	55

Both normoxic and hypoxic conditions revealed a consistent trend of apoptosis inhibition by Valsartan/LBQ, as evidenced by reduced cell viability at increasing drug concentrations. The IC₅₀ value in hypoxic conditions suggests enhanced sensitivity of cells to the drug in stressed environments. However, the limited scope of the experiments necessitates further research to validate these findings. These results suggest that Valsartan/LBQ has potential as an apoptosis inhibitor in endothelial cells, with dose-dependent effects evident under both normoxic and hypoxic conditions. Further studies are needed to confirm these results and explore the underlying mechanisms, as well as to evaluate the therapeutic relevance in vivo.

IV. DISCUSSION

The binding affinity of the IGFBP7-Sacubitril/Valsartan protein-ligand complex was analyzed using Autodock Vina. Due to limitations in the software, two separate models were constructed to account for both ligands. The most probable binding affinity was calculated as 5.6 kcal/mol for Valsartan and 6.2 kcal/mol for Sacubitril, with only the first mode out of the nine generate being considered in this study as it is the most probable. The preparation of proteins and ligands followed standard MGLTools protocols to ensure consistency in the docking environment. Additional validation was conducted by testing five other ligands (Isosorbide, Aspirin, Lisinopril, Acetaminophen, and Ibuprofen), which yielded an average binding affinity of 4.52 kcal/mol, notably lower than that of Sacubitril and Valsartan, confirming the unique binding properties of the latter two ligands. The binding site for the IGFBP7-ligand interaction was determined using PrankWeb, to predict the most probable binding site location and supported by conservation analysis, indicating high sequence stability in this region, which is often correlated with functional significance. Further validation was performed using COACH, a meta-server method incorporating TMSite and S-Site from the BioLiP database and PrDOS (Protein Disorder Prediction System) to assess disorderly regions of IGFBP7 likely to facilitate binding, affirming the most probable binding site location at around the high 150's on the amino acid chain. Results from the PLIP analysis indicate that Sacubitril formed nine hydrophobic interactions, three hydrogen bonds, and had a mean binding distance of 3.7 Å, with Valsartan forming the same number of hydrophobic interactions but only one hydrogen bond and two salt bridges. The median distance of hydrophobic interactions remained consistent at 3.7 Å. In the Bayesian network using GSE168742 (HFpEF), a clear trend is demonstrated in

upregulated IGFBP7 and HF. This result confirms the previous findings that upregulated IGFBP7 plays a detrimental factor in patients with HF (1). This network demonstrates roughly 89% of patients with HFpEF show upregulated levels of IGFBP7 as seen in Fig. 5, with a vast proportion, roughly 49% of all patients with HFpEF are within the fourth quartile, which is above 224.6 FPKM in concentration of IGFBP7. Furthermore, 98% of patients within the fourth quartile of IGFBP7 were afflicted by HFpEF, while only around 79% of patients in the first quartile were afflicted by HFpEF. This shows correlation between high amounts of IGFBP7 and HFpEF through the increased probability of higher levels of IGFBP7 being afflicted with HFpEF. This network was further applied to analyze IGFBP7's role in stroke, revealing a strong correlation between IGFBP7 upregulation and stroke pathology. Data from the GEO database (GSE221379) demonstrated that over 87.4% of stroke cases were associated with the highest quartile of IGFBP7 expression. This upregulation represented a threefold increase compared to control samples, with stroke-afflicted subjects exhibiting an average IGFBP7 expression of 285.45 FPKM versus 86.10 FPKM in controls. This demonstrates significant similarities in IGFBP7 expressions with the HFpEF dataset, which is interesting as it points towards a shared upstream problem which both of the diseases face. In-vitro experiments further explored the computational predictions. The dose-dependent inhibition of apoptosis by Sacubitril/Valsartan, as indicated by IC₅₀ values (~55 μ M), supports its role in modulating cellular survival mechanisms. Under hypoxic conditions, the sensitivity of endothelial cells to the drug examines its efficacy in stressed environments, akin to pathophysiological conditions seen in geriatric diseases such as stroke. As seen in other research papers, IGFBP7 plays a key role within cellular apoptosis and aging. This paper confirms the results that the controlled underexpression of IGFBP7 has a positive effect on HFpEF. IGFBP7 is also found in a consistently upregulation throughout Traumatic Brain Injuries (TBI), particularly in brain vasculature, highlighting its regulatory role in recovery and senescence [12]. Other machine learning approaches towards IGFBP7 show a particular result within the formation of abalone shells [21]. IGFBP7 is upregulated within the development of many animal and human tissues, demonstrating how it plays a role within cellular growth. These findings are significant as they strongly suggest that upregulated IGFBP7 is positively related to heart failure and other geriatric diseases. In this research, the mechanism of this interaction is further explored, meaning further research could be built upon this new information regarding the binding site, affinity, interactions, and concentrations. Establishing causation between IGFBP7 and HF is the next step for this research and would greatly benefit the current understanding of IGFBP7's effect on HF and geriatric diseases as a whole. New information on IGFBP7 has been discovered and now can be potentially used to conduct further research to eventually achieve the goal of understanding the connection between IGFBP7 as an upstream factor of

geriatric diseases, and to use it as a therapeutic target for a multitude of age related conditions. IGFBP7's involvement in cellular growth, apoptosis, and senescence pathways positions it as a critical upstream factor influencing geriatric disease. Sacubitril/Valsartan's ability to target IGFBP7 underscores its potential beyond HFpEF, extending to other conditions such as stroke and chronic vascular diseases. However, limitations in this study must be addressed. While computational and in-vitro results provide preliminary evidence, in-vivo experiments are essential for translating these findings into clinical applications. Additionally, expanding the Bayesian network to include datasets from other geriatric conditions could further elucidate IGFBP7's systemic role. Mechanistic studies investigating downstream effects of IGFBP7 modulation, such as its influence on oxidative stress and inflammatory pathways, are also necessary

V. CONCLUSION

The key findings that have been achieved through this experimentation is the positive correlation between IGFBP7 and other geriatric diseases. This sets IGFBP7 as a potential upstream factor that contributes to the detriment of these diseases in ways still undiscovered. IGFBP7 should be looked at as a potential therapeutic target not for just heart disease or stroke, but all types of geriatric diseases. The mechanisms in play here are not limited to just cardiovascular issues but the human body and aging as a whole. The more information there is on aging, the more ways diseases related to aging can be analyzed and potentially treated. There are many limitations of this experiment, as no real world experimentation was done to affirm the claims of the simulation. There will be more work to come in the following months on expanding the Bayesian network, connecting it to a variety of other geriatric diseases and biological pathways, as well as possible in vitro experiments.

CONFLICT OF INTEREST

The author declares no conflict of interest.

ACKNOWLEDGMENT

The author greatly appreciates Prof. Gil Alterovitz at MIT for the helpful discussion and mentorship for this research.

REFERENCES

- [1] T. To, S. Nomura, S. Yamada, *et al.*, "Cardiac fibroblasts regulate the development of heart failure via Htra3-TGF- β -IGFBP7 axis," *Nat. Commun.*, vol. 13, 3275, 2022.
- [2] J. Januzzi Jr, M. Packer, B. Claggett, *et al.*, "IGFBP7 (insulin-like-growth-factor binding-protein-7) and neprilysin inhibition in patients with heart failure," *Circulation: Heart Failure*, vol. 11, no. 10, e005133, Oct. 2018.
- [3] J. Li, S. Fan, W. Michael, and S. Consolato, "Insulin growth factor binding protein 7 (IGFBP7)-related cancer and IGFBP3 and IGFBP7 crosstalk," *Frontiers in Oncology*, vol. 10, 2020.
- [4] N. Wajapeyee, R. W. Serra, X. Zhu, *et al.*, "Role of IGFBP7 in senescence induction by BRAF," *Cell*, vol. 132, no. 3, Feb. 2010.
- [5] N. Wajapeyee, R. W. Serra, X. Zhu, *et al.*, "Oncogenic BRAF induces senescence and apoptosis through pathways mediated by the secreted protein IGFBP7," *Cell*, vol. 141, no. 5, Feb. 2008.
- [6] D. Kultz, "Molecular and evolutionary basis of the cellular stress response," *Annual Review of Physiology*, vol. 67, Mar. 2005.
- [7] E. Willighagen, WikiPathways, Source 15767, Dec. 22.
- [8] E. Kaplinsky, "Sacubitril/valsartan in heart failure: Latest evidence and place in therapy," *Therapeutic Advances in Chronic Disease*, vol. 7, no. 6, pp. 278–290, 2016. doi: 10.1177/2040622316665350
- [9] E. Esmeijer, A. Schoe, L. R. Ruhaak, *et al.*, "The predictive value of TIMP-2 and IGFBP7 for kidney failure and 30-day mortality after elective cardiac surgery," *Sci. Rep.*, vol. 11, 1071, 2021.
- [10] V. Bracun, B. Essen, A. Voors, *et al.*, "Insulin-like growth factor binding protein 7 (IGFBP7), a link between heart failure and senescence," *ESC Heart Failure*, vol. 9, no. 6, pp. 4167–4176, Sep. 2022.
- [11] L. Zhang, D. Smyth, M. Al-Khalaf, *et al.*, "Insulin-like growth factor-binding protein-7 (IGFBP7) links senescence to heart failure," *Nat. Cardiovasc Res.*, vol. 1, pp. 1195–1214, 2022.
- [12] J. Wang, X. Deng, Y. Xie, *et al.*, "An integrated transcriptome analysis reveals IGFBP7 upregulation in vasculature in traumatic brain injury," *Frontiers in Genetics*, vol. 11, 2021.
- [13] National Center for Biotechnology Information (NCBI), GEO Dataset GSE168742, 2021.
- [14] PrankWeb, PrankWeb: Predicting Ligand Binding Sites Using Machine Learning, 2021.
- [15] Bnlearn, bnlearn: Bayesian Network Structure Learning and Parameter Learning, 2021.
- [16] Novartis Pharma AG, Valsartan/LBQ, 2021.
- [17] MedChemExpress, LCZ696, 2021.
- [18] Cell Biologics, C57BL/6 Mouse Primary Brain Microvascular Endothelial Cells, 2021.
- [19] BioSpherix, Hypoxia Workbench (X3 Xvivo System), 2021.
- [20] COACH, COACH: Ligand Binding Site Prediction, 2021.
- [21] G. Wang, N. Li, L. Zhang, *et al.*, "IGFBP7 promotes hemocyte proliferation in small abalone *Haliotis diversicolor*, proved by dsRNA and cap mRNA exposure," *Gene*, vol. 571, no. 1, pp. 65–70, 2015.

Copyright © 2025 by the authors. This is an open access article distributed under the Creative Commons Attribution License which permits unrestricted use, distribution, and reproduction in any medium, provided the original work is properly cited ([CC BY 4.0](https://creativecommons.org/licenses/by/4.0/)).